

Ratiometric fluorescence *off-on-off* sensor for Cu²⁺ in aqueous buffer by a lower rim triazole linked benzimidazole conjugate of calix[4]arene

Rakesh Kumar Pathak,^a Vijaya Kumar Hinge,^b Prasenjit Mondal^a and Chebrolu Pulla Rao^{a,b*}

^aBioinorganic Laboratory & Department of Chemistry, ^bDepartment of Biosciences & Bioengineering,
Indian Institute of Technology Bombay, Powai, Mumbai 400 076, India

Contents

Figure S1. ¹ H NMR, ¹³ C NMR and HR Mass Spectra for L	02
Figure S2. Schematic diagram showing the hydrogen bonding pattern for L	05
Figure S3. Fluorescence spectra for the titration of control molecule 3	06
Figure S4. Minimum detection limit experiment for L with Cu ²⁺ in different solvent systems	06
Figure S5. Fluorescence spectra for the titration of L with Cu ²⁺ in ethanol	06
Figure S6. Fluorescence spectra for the titration of L with Cu ²⁺ in different solvents	07
Figure S7. Effect of solvent polarity on the excimer band at 380 nm	07
Figure S8. Fluorescence titrations with ethidium bromide (EtBr)	07
Figure S9. Absorption spectra for the titration of L with Cu ²⁺ in aqueous buffer	08
Figure S10. Job's plot for the L with Cu ²⁺	08
Figure S11. Visual color change for the interaction of L with Cu ²⁺ during the EPR titrations	09
Figure S12. Absorption spectra measured for the samples that were used for EPR	10
Figure S13. ¹ H NMR spectra for the titration of L with Cu ²⁺ in DMSO-d ₆ and CD ₃ OD	11
Figure S14. High resolution mass spectra of L with Cu ²⁺	12
Figure S15. Pictorial representation for the MOs present on L and [L' (Cu)] ²⁺	19
Table S1. - S2. Selected bond lengths and bond angles for L	3-4
Table S3. Hydrogen bond length and bond angle data for L .	5
Table S4. Conformational angles (°) of the arms obtained upon optimization	13
Table S5. Cartesian coordinates for B3LYP/6-31G optimized structure of L'	14
Table S6. Cartesian coordinates for B3LYP/6-31G(d,p) optimized structure of [L' (Cu)] ²⁺	15
Table S7. Cartesian coordinates for B3LYP/6-31G(d,p) optimized structure of [L' _{-2H} (Cu) ₂] ²⁺	17
Table S8. Percentage of MOs present on the fragments of L' , [L' (Cu)] ²⁺ and [L' _{-2H} (Cu) ₂] ²⁺	19

^1H NMR, ^{13}C NMR and ESI MS spectra of **L**.

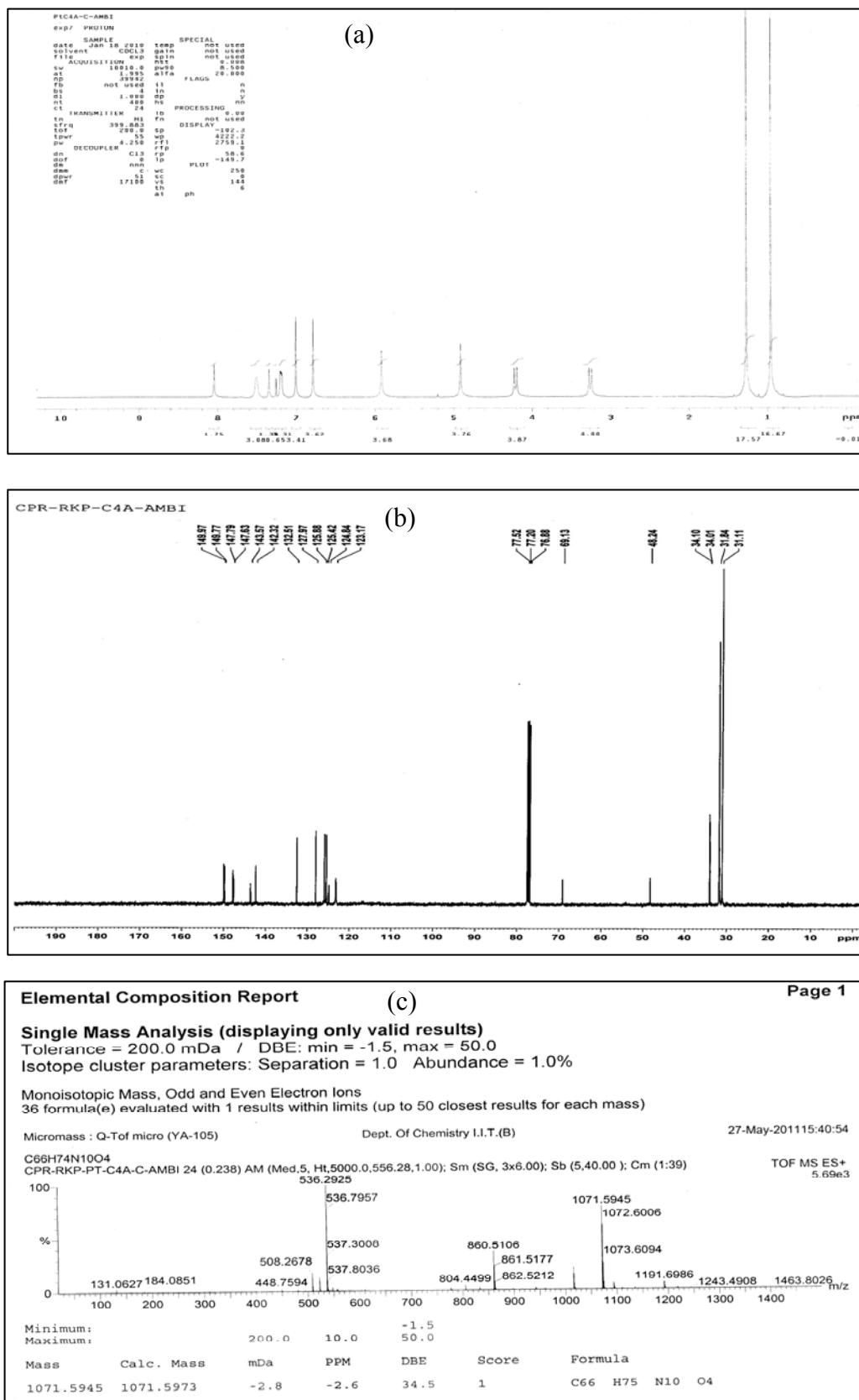


Figure S1. Spectra of **L**: (a) ^1H NMR; (b) ^{13}C NMR and (c) ESI HRMS.

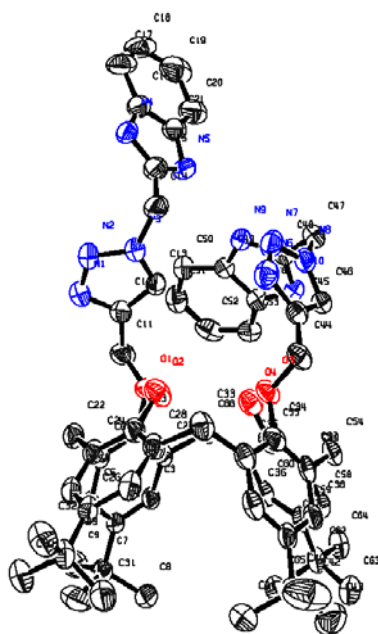


Table S1. Selected bond lengths for **L**

O(1)-C(1)	1.395(5)	C(20)-C(21)	1.370(8)	C(62)-C(63)	1.531(7)
O(1)-C(11)	1.450(5)	C(22)-C(24)	1.515(6)	C(62)-C(65)	1.544(7)
O(2)-C(23)	1.352(6)	C(23)-C(24)	1.397(6)	O(102)-C(333)	1.402(7)
O(3)-C(34)	1.397(6)	C(23)-C(28)	1.399(7)	O(103)-C(101)	1.412(11)
O(3)-C(44)	1.440(5)	C(24)-C(25)	1.396(7)	C(102)-O(101)	1.437(8)
O(4)-C(55)	1.381(5)	C(25)-C(26)	1.388(7)	C(55)-C(57)	1.388(6)
N(1)-N(2)	1.315(6)	C(26)-C(27)	1.404(6)	C(55)-C(61)	1.406(6)
N(1)-C(12)	1.354(6)	C(26)-C(29)	1.516(7)	C(57)-C(58)	1.383(6)
N(2)-N(3)	1.330(5)	C(27)-C(28)	1.399(7)	C(58)-C(59)	1.396(6)
N(3)-C(13)	1.334(5)	C(28)-C(33)	1.500(6)	C(59)-C(60)	1.413(6)
N(3)-C(14)	1.475(6)	C(29)-C(31)	1.520(7)	C(59)-C(62)	1.522(7)
N(4)-C(15)	1.308(6)	C(29)-C(32)	1.528(7)	C(60)-C(61)	1.379(6)
N(4)-C(16)	1.378(7)	C(29)-C(30)	1.525(7)	C(61)-C(66)	1.517(6)
N(5)-C(15)	1.368(7)	C(33)-C(35)	1.531(6)	C(62)-C(64)	1.522(7)
N(5)-C(21)	1.378(7)	C(34)-C(39)	1.393(6)	C(7)-C(8)	1.540(6)
N(6)-C(45)	1.378(6)	C(34)-C(35)	1.404(7)	C(11)-C(12)	1.482(7)
N(7)-N(8)	1.334(5)	C(35)-C(36)	1.381(7)	C(12)-C(13)	1.354(6)
N(8)-C(46)	1.341(6)	C(36)-C(37)	1.404(6)	C(14)-C(15)	1.490(8)
N(8)-C(47)	1.466(6)	C(37)-C(38)	1.378(7)	C(16)-C(17)	1.373(7)
N(9)-C(48)	1.337(5)	C(37)-C(40)	1.528(7)	C(16)-C(21)	1.421(8)
N(9)-C(49)	1.395(6)	C(38)-C(39)	1.387(7)	C(17)-C(18)	1.366(10)
N(10)-C(48)	1.342(6)	C(39)-C(54)	1.519(7)	C(18)-C(19)	1.427(10)
N(10)-C(56)	1.382(6)	C(40)-C(42)	1.506(9)	C(19)-C(20)	1.403(8)
C(1)-C(6)	1.386(6)	C(40)-C(41)	1.532(7)	C(52)-C(53)	1.377(7)
C(1)-C(2)	1.406(6)	C(40)-C(43)	1.565(8)	C(53)-C(56)	1.385(7)
C(2)-C(3)	1.382(6)	C(44)-C(45)	1.467(7)	C(54)-C(57)	1.515(6)
C(2)-C(66)	1.529(6)	C(45)-C(46)	1.372(7)	C(6)-C(22)	1.509(6)
C(3)-C(4)	1.392(6)	C(47)-C(48)	1.478(7)	C(7)-C(9)	1.529(7)
C(4)-C(5)	1.388(6)	C(49)-C(50)	1.385(6)	C(7)-C(10)	1.526(7)
C(4)-C(7)	1.529(6)	C(49)-C(56)	1.409(6)	C(51)-C(52)	1.408(7)
C(50)-C(51)	1.383(7)	C(5)-C(6)	1.411(6)		

Table S2. Selected bond angles for **L**

C(1)-O(1)-C(11)	114.1(3)	N(5)-C(15)-C(14)	122.6(4)	C(38)-C(39)-C(54)	119.8(4)
C(34)-O(3)-C(44)	113.7(3)	N(4)-C(16)-C(17)	129.4(6)	C(34)-C(39)-C(54)	121.1(4)
N(2)-N(1)-C(12)	109.2(4)	N(4)-C(16)-C(21)	109.6(4)	C(42)-C(40)-C(41)	108.7(5)
N(1)-N(2)-N(3)	106.5(4)	C(17)-C(16)-C(21)	121.0(6)	C(42)-C(40)-C(37)	110.7(5)
N(2)-N(3)-C(13)	111.3(4)	C(18)-C(17)-C(16)	117.0(6)	C(41)-C(40)-C(37)	110.3(4)
N(2)-N(3)-C(14)	119.5(4)	C(17)-C(18)-C(19)	122.7(6)	C(42)-C(40)-C(43)	109.9(5)
C(13)-N(3)-C(14)	129.2(4)	C(20)-C(19)-C(18)	120.3(7)	C(41)-C(40)-C(43)	104.3(5)
C(15)-N(4)-C(16)	105.0(5)	C(21)-C(20)-C(19)	115.9(6)	C(37)-C(40)-C(43)	112.6(4)
C(15)-N(5)-C(21)	106.2(4)	C(20)-C(21)-N(5)	131.7(5)	O(3)-C(44)-C(45)	107.8(4)
N(7)-N(6)-C(45)	109.0(4)	C(20)-C(21)-C(16)	123.1(5)	C(46)-C(45)-N(6)	107.1(4)
N(6)-N(7)-N(8)	107.5(4)	N(5)-C(21)-C(16)	105.2(5)	C(46)-C(45)-C(44)	129.7(4)
N(7)-N(8)-C(46)	111.2(4)	C(24)-C(22)-C(6)	111.8(3)	N(6)-C(45)-C(44)	123.2(5)
N(7)-N(8)-C(47)	119.5(4)	O(2)-C(23)-C(24)	123.8(4)	N(8)-C(46)-C(45)	105.2(4)
C(46)-N(8)-C(47)	128.8(4)	O(2)-C(23)-C(28)	115.7(4)	N(8)-C(47)-C(48)	109.8(4)
C(48)-N(9)-C(49)	104.5(4)	C(24)-C(23)-C(28)	120.4(5)	N(9)-C(48)-N(10)	112.9(4)
C(48)-N(10)-C(56)	108.1(4)	C(25)-C(24)-C(23)	118.4(4)	N(9)-C(48)-C(47)	123.2(4)
C(6)-C(1)-O(1)	117.9(4)	C(25)-C(24)-C(22)	120.1(4)	N(10)-C(48)-C(47)	123.6(4)
C(6)-C(1)-C(2)	122.2(4)	C(23)-C(24)-C(22)	121.5(4)	C(50)-C(49)-N(9)	129.7(4)
O(1)-C(1)-C(2)	119.7(4)	C(26)-C(25)-C(24)	123.7(4)	C(50)-C(49)-C(56)	120.6(4)
C(3)-C(2)-C(1)	117.1(4)	C(25)-C(26)-C(27)	115.9(5)	N(9)-C(49)-C(56)	109.7(4)
C(3)-C(2)-C(66)	120.3(4)	C(25)-C(26)-C(29)	124.0(4)	C(51)-C(50)-C(49)	118.0(4)
C(1)-C(2)-C(66)	122.5(4)	C(27)-C(26)-C(29)	120.1(4)	C(50)-C(51)-C(52)	120.8(5)
C(2)-C(3)-C(4)	123.1(4)	C(28)-C(27)-C(26)	122.8(4)	C(53)-C(52)-C(51)	121.7(5)
C(5)-C(4)-C(3)	117.9(4)	C(27)-C(28)-C(23)	118.7(4)	C(52)-C(53)-C(56)	117.2(4)
C(5)-C(4)-C(7)	121.2(4)	C(27)-C(28)-C(33)	120.0(4)	C(57)-C(54)-C(39)	113.6(4)
C(3)-C(4)-C(7)	121.0(4)	C(23)-C(28)-C(33)	121.1(4)	N(10)-C(56)-C(53)	133.5(4)
C(4)-C(5)-C(6)	121.6(4)	C(26)-C(29)-C(31)	110.7(4)	N(10)-C(56)-C(49)	104.8(4)
C(1)-C(6)-C(5)	117.8(4)	C(26)-C(29)-C(32)	109.9(4)	C(53)-C(56)-C(49)	121.7(4)
C(1)-C(6)-C(22)	122.3(4)	C(31)-C(29)-C(32)	108.2(5)	O(4)-C(55)-C(57)	123.4(4)
C(5)-C(6)-C(22)	119.7(4)	C(26)-C(29)-C(30)	112.7(4)	O(4)-C(55)-C(61)	115.5(4)
C(4)-C(7)-C(9)	108.4(4)	C(31)-C(29)-C(30)	107.5(4)	C(57)-C(55)-C(61)	121.1(4)
C(4)-C(7)-C(10)	111.9(4)	C(32)-C(29)-C(30)	107.6(4)	C(58)-C(57)-C(55)	118.3(4)
C(9)-C(7)-C(10)	109.2(4)	C(28)-C(33)-C(35)	109.8(4)	C(58)-C(57)-C(54)	119.0(4)
C(4)-C(7)-C(8)	110.3(4)	C(39)-C(34)-O(3)	119.2(4)	C(55)-C(57)-C(54)	122.7(4)
C(9)-C(7)-C(8)	109.4(4)	C(39)-C(34)-C(35)	120.9(4)	C(57)-C(58)-C(59)	123.7(4)
C(10)-C(7)-C(8)	107.6(4)	O(3)-C(34)-C(35)	119.7(4)	C(58)-C(59)-C(60)	115.6(4)
O(1)-C(11)-C(12)	107.2(4)	C(36)-C(35)-C(34)	117.5(4)	C(58)-C(59)-C(62)	124.3(4)
N(1)-C(12)-C(13)	107.8(4)	C(36)-C(35)-C(33)	120.3(4)	C(60)-C(59)-C(62)	120.1(4)
N(1)-C(12)-C(11)	122.1(4)	C(34)-C(35)-C(33)	122.0(4)	C(61)-C(60)-C(59)	123.0(4)
C(13)-C(12)-C(11)	130.0(4)	C(35)-C(36)-C(37)	123.2(5)	C(60)-C(61)-C(55)	118.3(4)
N(3)-C(13)-C(12)	105.3(4)	C(38)-C(37)-C(36)	117.0(4)	C(60)-C(61)-C(66)	120.8(4)
N(3)-C(14)-C(15)	109.3(4)	C(38)-C(37)-C(40)	123.2(4)	C(55)-C(61)-C(66)	120.8(4)
N(4)-C(15)-N(5)	114.0(5)	C(36)-C(37)-C(40)	119.7(4)	C(59)-C(62)-C(64)	109.9(4)
N(4)-C(15)-C(14)	123.5(5)	C(37)-C(38)-C(39)	122.4(4)	C(59)-C(62)-C(63)	112.1(4)
C(63)-C(62)-C(65)	107.1(4)	C(38)-C(39)-C(34)	119.0(4)	C(64)-C(62)-C(63)	108.6(4)
C(61)-C(66)-C(2)	109.2(4)	C(64)-C(62)-C(65)	109.3(4)	C(59)-C(62)-C(65)	109.8(3)

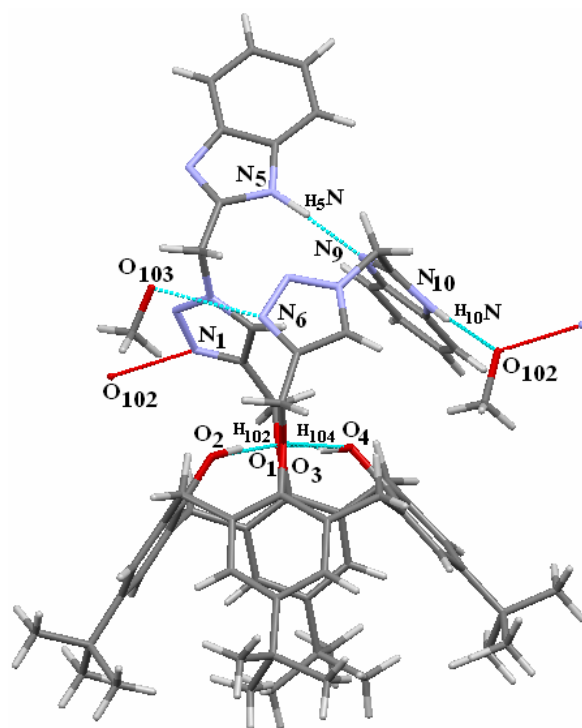


Figure S2: Schematic diagram shows the hydrogen bonding pattern for **L**.

Table S3. Hydrogen bond length and bond angle data for **L**.

D – H ... A	D – H (Å)	A ... H (Å)	D ... A (Å)	D – H – A (°)
O4 – H104 ... O3	1.05 (7)	1.67 (7)	2.706 (4)	165 (6)
O2 – H102 ... O1	1.02 (6)	1.70 (7)	2.712 (4)	167 (5)
N10 – H10N ... O102	0.80 (4)	1.96 (4)	2.755 (4)	175 (5)
N5 – H5N ... N9	1.07 (3)	1.79 (3)	2.857 (4)	171 (4)

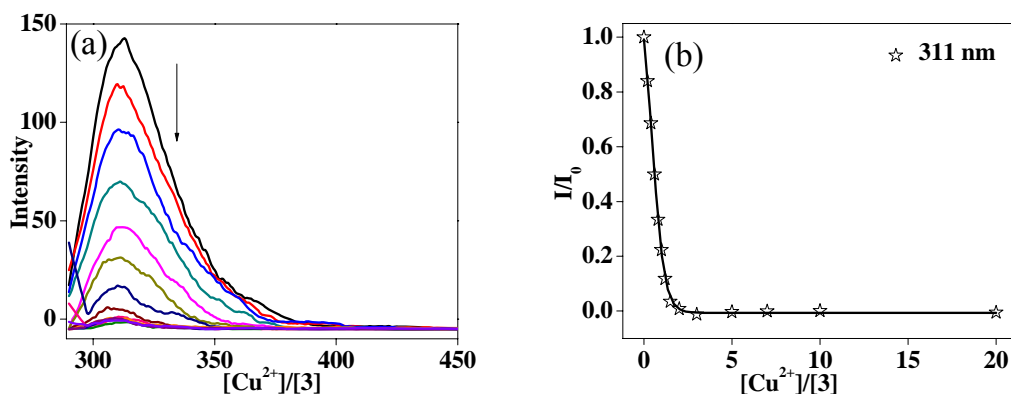


Figure S3: (a) Fluorescence spectra obtained during the titration of control molecule **3** in methanol. (b) relative fluorescence intensity (I/I_0) as a function of $[Cu^{2+}]/[3]$ mole ratio.

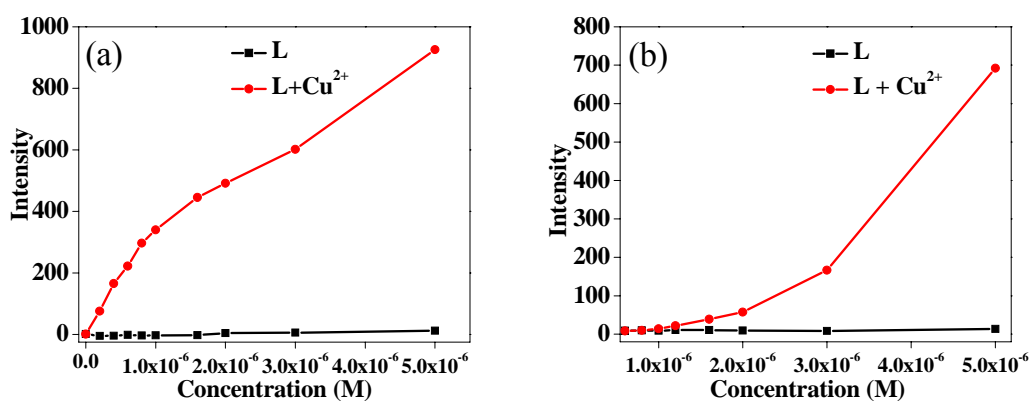


Figure S4: Fluorescence spectra obtained during the titration of **L** in (a) methanol and (b) aqueous-buffer medium by keeping ligand to Zn^{2+} ratio as 1:1. This is used for obtaining the minimum detection of limit of Cu^{2+} by **L**.

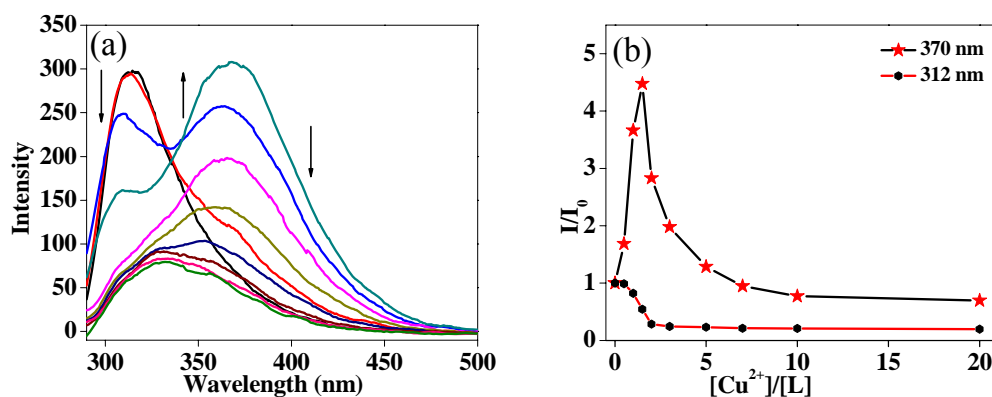


Figure S5: (a) Fluorescence spectra obtained during the titration of **L** with Cu^{2+} in ethanol; $\lambda_{ex} = 280$ nm; (b) relative fluorescence intensity (I/I_0) as a function of $[Cu^{2+}]/[L]$ mole ratio.

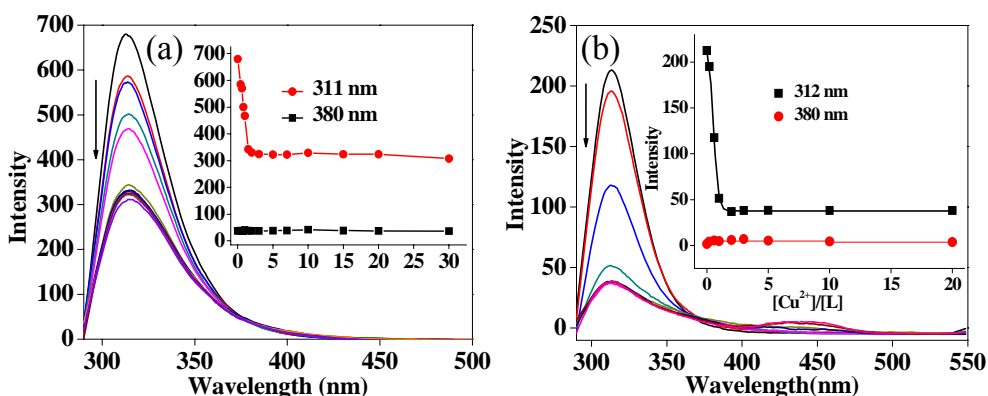


Figure S6: Fluorescence spectra obtained during the titration of **L** with Cu^{2+} in different solvent systems; (a) tetrahydrofuran; (b) acetonitrile; $\lambda_{\text{ex}} = 280 \text{ nm}$. Inset of both shows relative fluorescence intensity (I/I_0) as a function of $[\text{Cu}^{2+}]/[\text{L}]$ mole ratio.

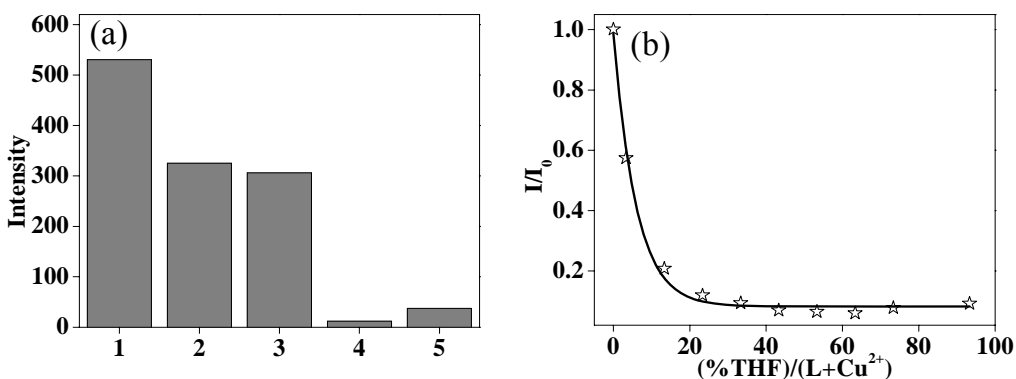


Figure S7: The effect of solvent polarity on the excimer band of 380 nm (a) Histogram showing the fluorescence intensity observed in the titration of **L** with Cu^{2+} in different solvent systems: (1) methanol, (2) aqueous-buffer-medium, (3) ethanol, (4) acetonitrile and (5) tetrahydrofuran; (b) relative fluorescence intensity (I/I_0) as a function of $[\% \text{ of THF}]/[\text{L} + \text{Cu}^{2+}]$ mole ratio $\{[\text{L}] = 10 \mu\text{M}, [\text{Cu}^{2+}] = 30 \mu\text{M}; \lambda_{\text{ex}} = 280 \text{ nm}\}$.

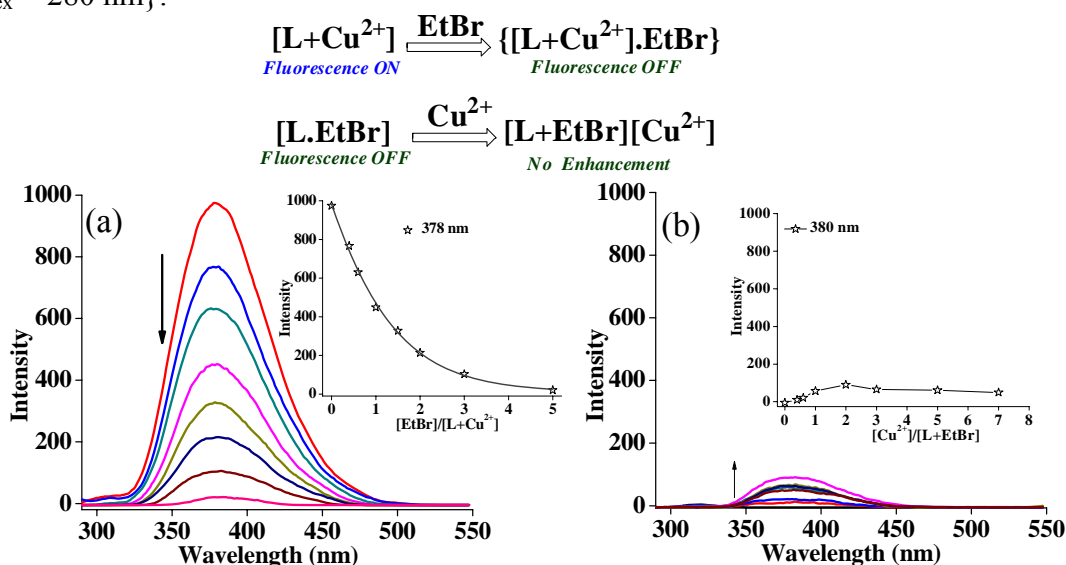


Figure S8: Fluorescence titrations with ethidium bromide (EtBr): (a) spectra obtained during the titration of $\{[\text{L} + \text{Cu}^{2+}] + \text{EtBr}\}$, inset shows the fluorescence intensity (I) as a function of $[\text{EtBr}]/[\text{L} + \text{Cu}^{2+}]$ mole ratio. (b) spectra obtained during the titration of $\{[\text{L} + \text{EtBr}] + \text{Cu}^{2+}\}$, inset shows the fluorescence intensity (I) as a function of $[\text{Cu}^{2+}]/[\text{L} + \text{EtBr}]$ mole ratio in methanol. $\lambda_{\text{ex}} = 280 \text{ nm}$. $[\text{L}] = 10 \mu\text{M}$.

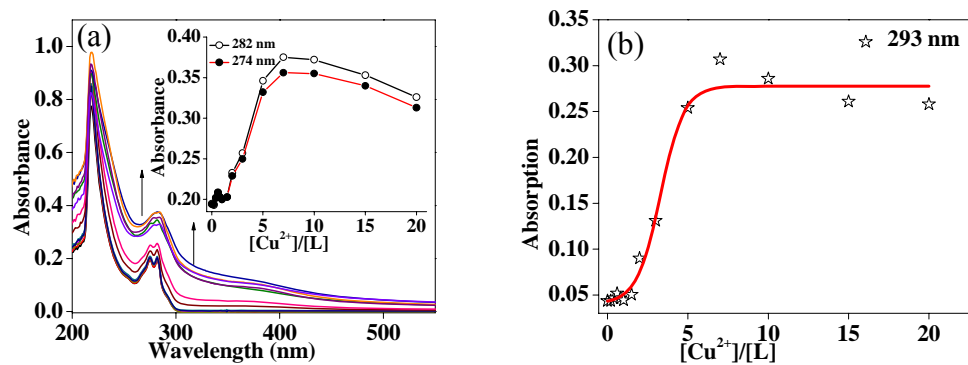


Figure S9: (a) Absorption spectra obtained during the titration **L** with Cu²⁺ in aqueous-buffer medium; inset shows the plot of absorbance vs. [Cu²⁺]/ [L] for 274 and 282 nm absorption bands; (b) plot of absorbance vs. [Cu²⁺]/ [L] for 293 nm absorption band.

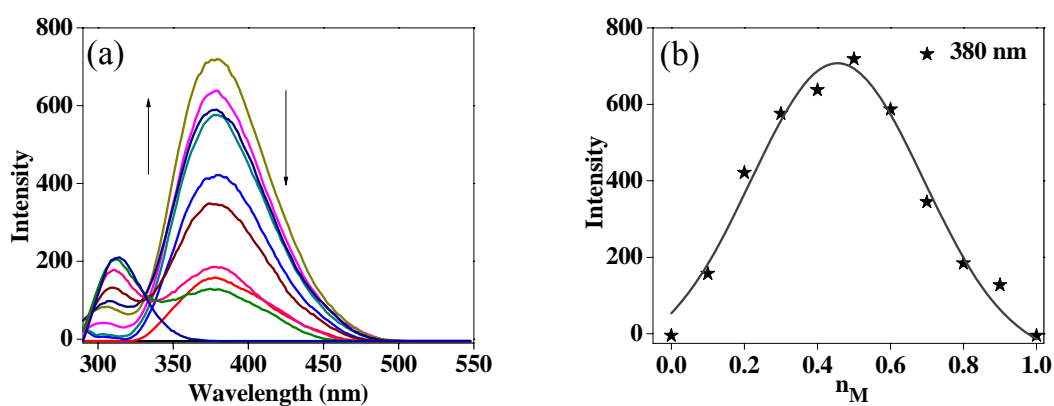


Figure S10: Job's plot for the **L** with Cu²⁺ for 1:2 ligand to metal binding. Concentration for **L** was 6 x 10⁻⁴ M whereas the concentration for Cu²⁺ was 12 x 10⁻⁴ M; (a) fluorescence intensity plot; (b) plot of fluorescence intensity as a function of the mole fraction of the metal ion.

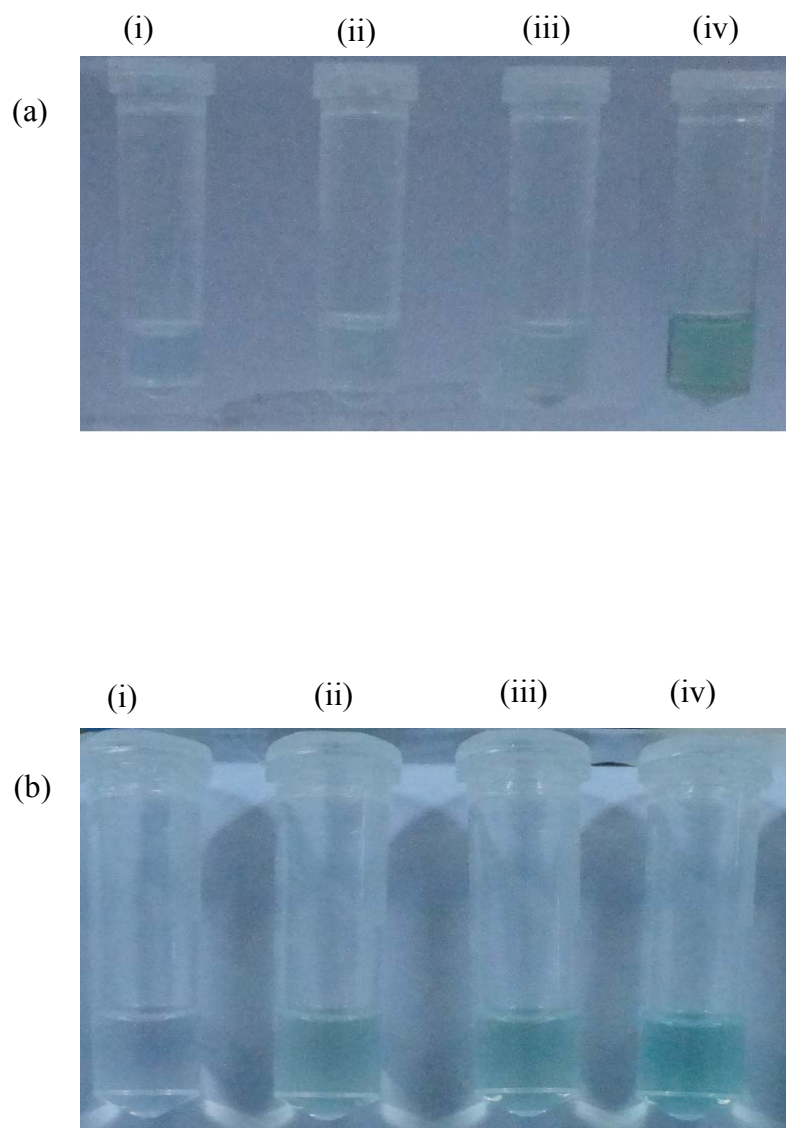


Figure S11: Visual colour change observed for the interaction of **L** with Cu^{2+} during the EPR titrations: (a) observed colour change when **L** was titrated with varying amount of Cu^{2+} (in first set of EPR samples) (i) 0, (ii) 0.25, (iii) 0.5, and (iv) 1.0 equiv. of Cu^{2+} .; (b) observed colour change when Cu^{2+} was titrated with varying amount of **L** (second set of EPR samples) (i) 0, (ii) 0.25, (iii) 0.5, and (iv) 1.0 equiv. of **L**.

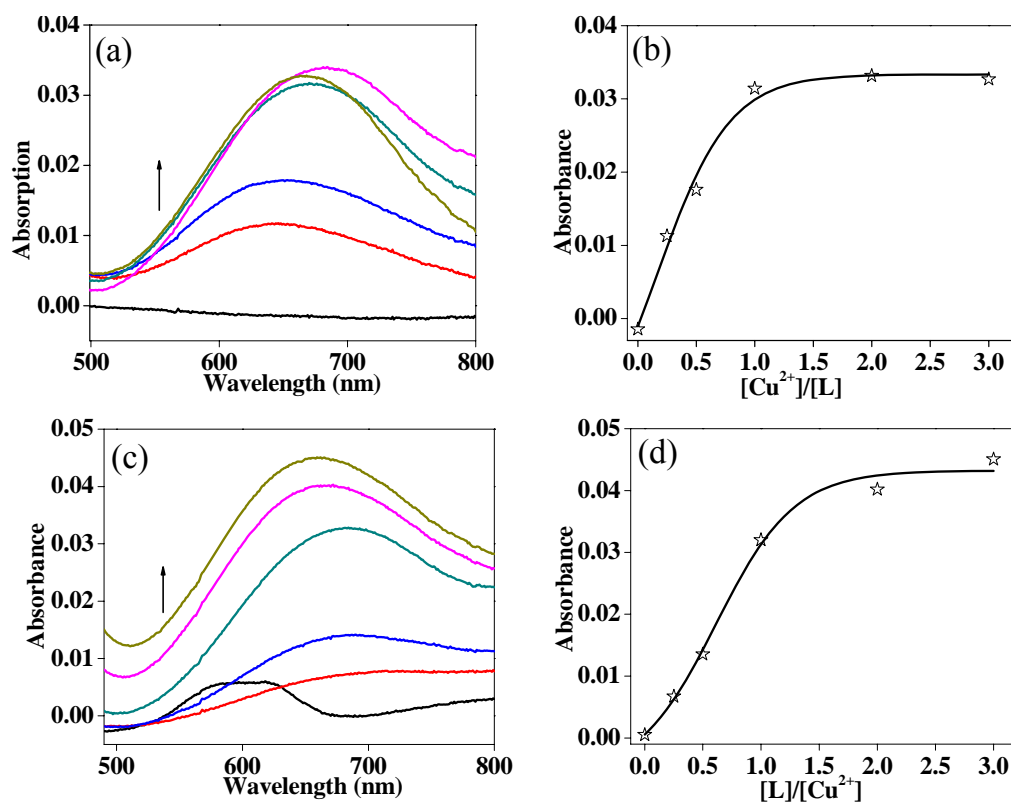


Figure S12: Absorption spectral measurements made with the samples that were used for EPR: (a) spectral traces obtained in the $d \rightarrow d$ transition region 500 – 800 nm when **L** was titrated with varying amounts of Cu^{2+} . (b) Plot of absorbance vs. $[\text{Cu}^{2+}]/[\text{L}]$ for the $d \rightarrow d$ band observed at 665 nm. (c) Spectral traces observed in the $d \rightarrow d$ transition region 500 – 800 nm when Cu^{2+} was titrated with varying amount of **L**. (d) Plot of absorbance vs. $[\text{L}]/[\text{Cu}^{2+}]$ for the $d \rightarrow d$ band at 665 nm.

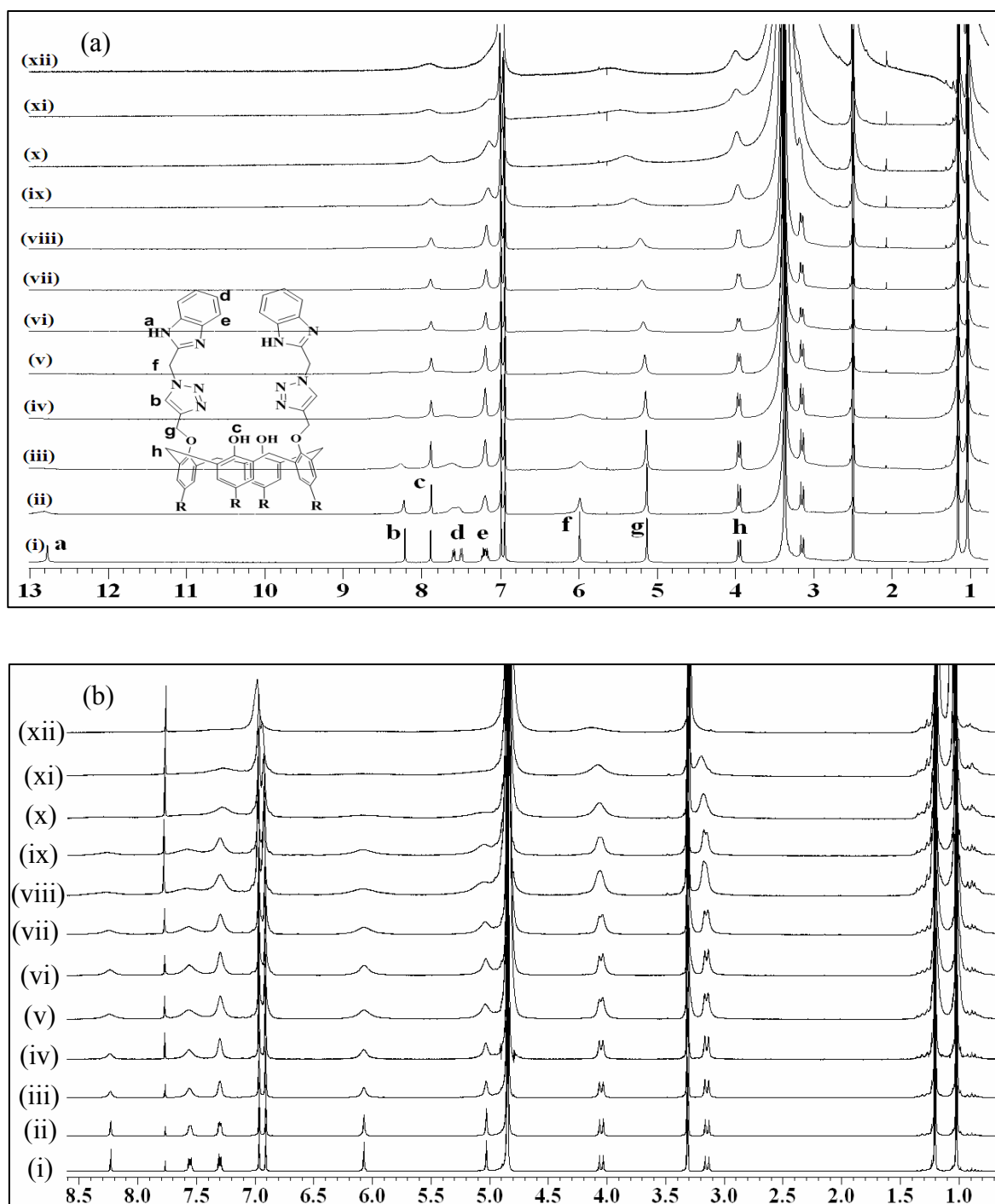


Figure S13: ^1H NMR spectra measured during the titration of **L** with different mole ratio of Cu^{2+} in (a) DMSO-d_6 and (b) CD_3OD (minimum amount of CDCl_3 ; $[\text{Cu}]/[\text{L}]$ ratios are, (i) 0; (ii) 0.0125; (iii) 0.025; (iv) 0.0375; (v) 0.05; (vi) 0.0625; (vii) 0.075; (viii) 0.1; (ix) 0.125; (x) 0.187; (xi) 0.25; (xii) 0.5; a = benzimidazole-NH; b = triazole-H, c = phenolic-OH, d,e = benzimidazole Ar-H, f,g,h = bridged CH_2 protons. R = *tert* butyl. Spectra obtained at >0.5 equivalents of Cu^{2+} were not shown because of complete broadening of the NMR signals

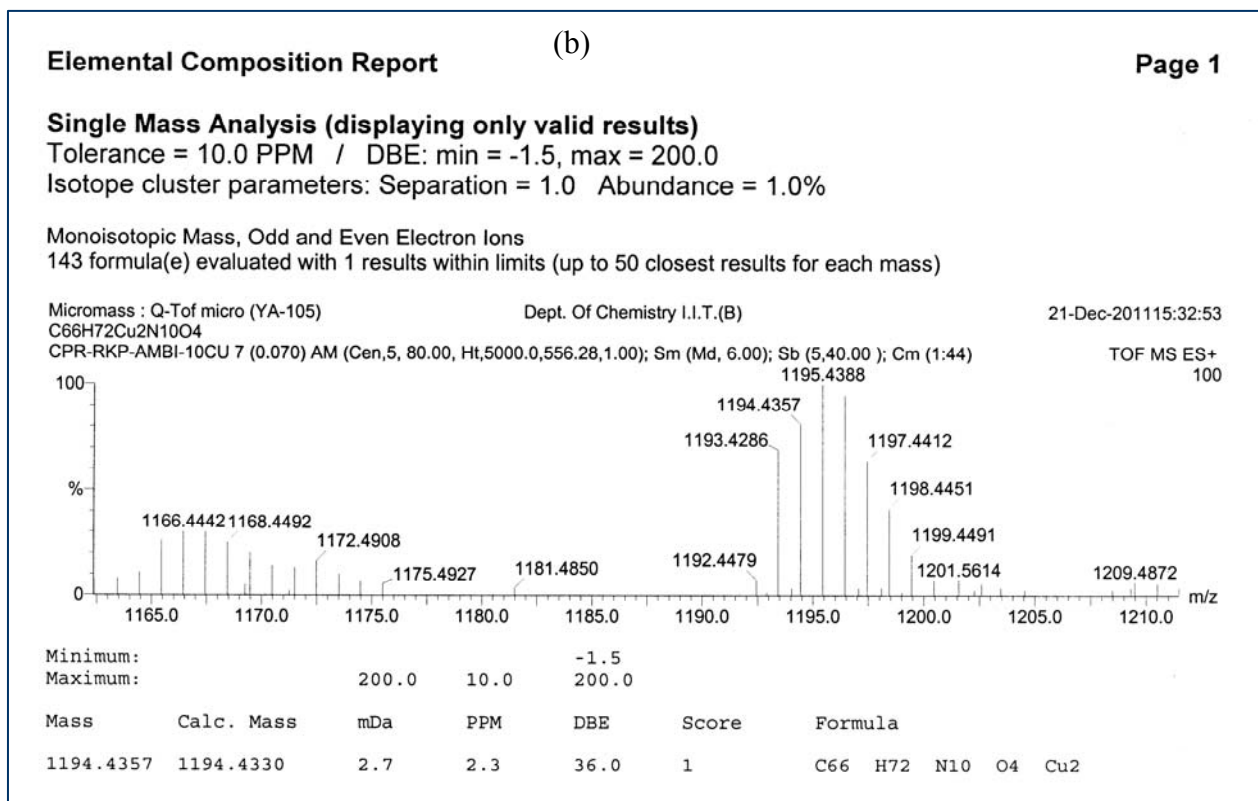
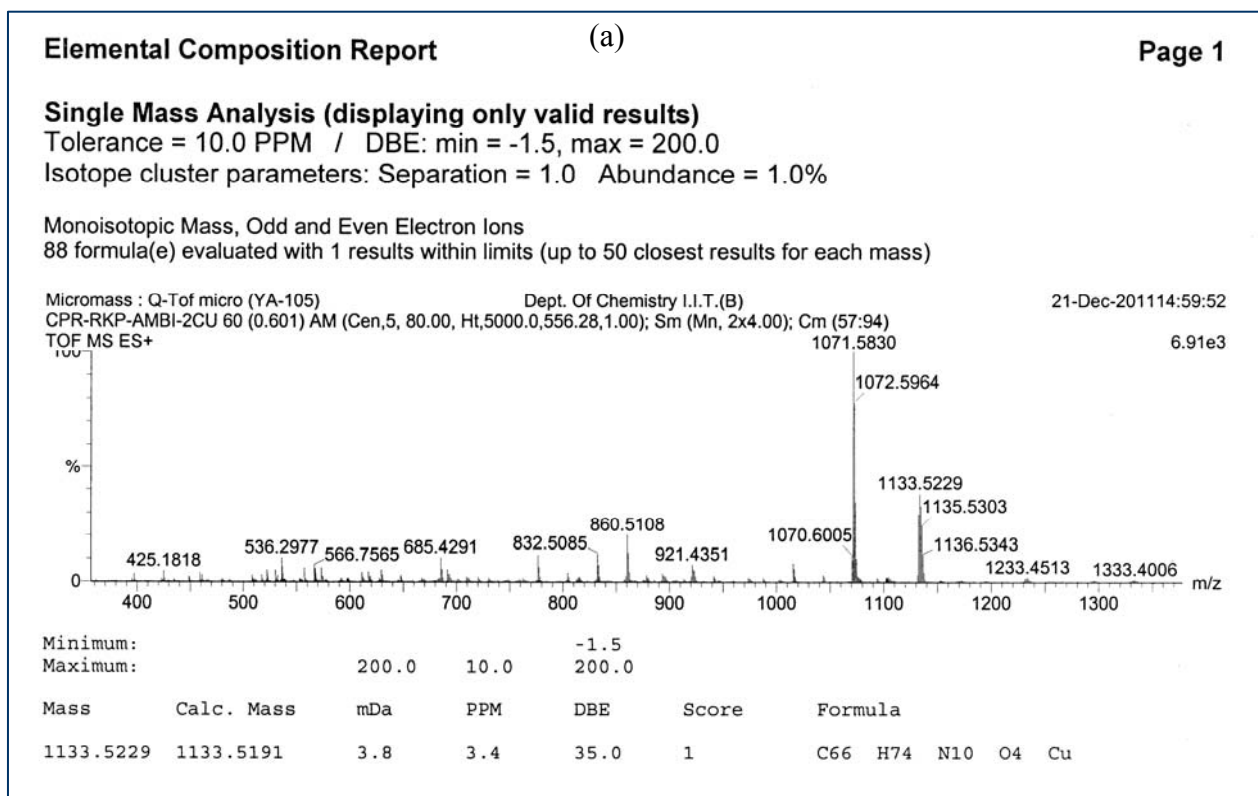
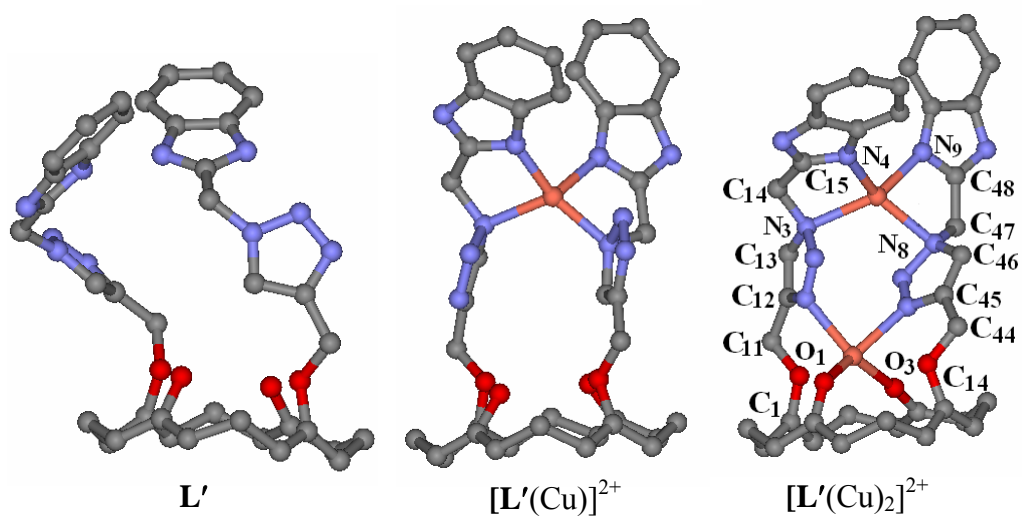


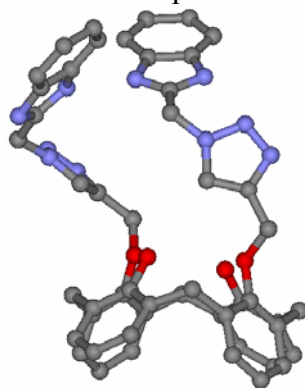
Figure S14: High resolution mass spectra of **L** with Cu^{2+} : (a) 1:1 [**L**:Cu]; (b) 1:2 [**L** : 2Cu].

Table S4. Conformational angles (°) of the arms obtained upon optimization of **L'**, and its Cu²⁺ complexes, viz., [L'(Cu)]²⁺ and [L'(Cu)₂]²⁺.



Atoms	Dihedral Angle (°)		
	L' (Optimized structure)	[L'(Cu)] ²⁺	[L'(Cu) ₂] ²⁺
C1-O1-C11-C12	107.051	175.5	175.245
O1-C11-C12-C13	36.219	126.7	151.761
C11-C12-C13-N3	179.584	-173.9	177.626
C12-C13-N3-C14	174.759	-118.8	-124.232
C13-N3-C14-C15	58.726	-168.0	-176.945
N3-C14-C15-N4	-140.387	28.8	35.116
C34-O3-C44-C45	-160.145	161.1	130.912
O3-C44-C45-C46	39.964	-15.7	-177.228
C44-C45-C46-N8	178.275	-178.3	177.745
C45-C46-N8-C47	-176.712	119.3	-135.683
C46-N8-C47-C48	-125.059	172.7	-97.336
N8-C47-C48-N9	147.948	-18.5	-31.624

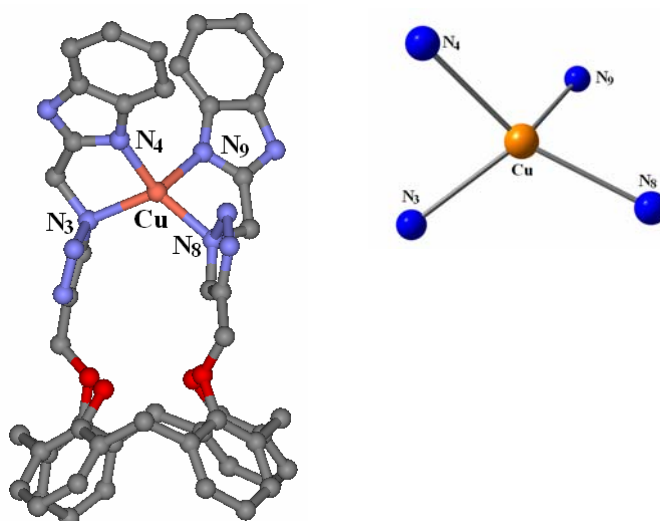
Table S5. Cartesian coordinates for B3LYP/6-31G optimized structure of **L'**.



Z	Coordinates			Z	Coordinates		
	x	y	z		x	y	z
8	-1.08989	0.29968	1.785631	1	-1.36688	-3.02867	3.572212
8	-1.1035	-1.50808	-0.10167	6	-1.86298	-2.63616	0.206585
8	-2.40034	0.215426	-2.45123	6	-1.99552	-3.10882	1.532095
8	-2.62885	1.801918	-0.324	6	-2.67012	-4.32152	1.741565
7	2.063504	1.191194	3.409936	1	-2.76442	-4.69894	2.755934
7	3.125503	0.423458	3.609164	6	-3.19955	-5.05316	0.676722
7	2.978245	-0.68389	2.785044	6	-3.09695	-4.54534	-0.62028
7	4.843426	-3.38785	1.215311	1	-3.5237	-5.09948	-1.45156
7	5.038708	-1.20319	0.637119	6	-2.45498	-3.3245	-0.87314
7	0.535846	1.548755	-4.05497	6	-2.48079	-2.71866	-2.27318
7	1.770036	1.525152	-3.5672	1	-2.49212	-3.53186	-3.00919
7	1.773942	0.589743	-2.53563	1	-1.57709	-2.13344	-2.43622
7	4.336753	1.488793	-0.06121	6	-3.6602	-0.44012	-2.53301
7	3.580419	2.768437	-1.75093	6	-3.71844	-1.84341	-2.48947
6	-2.18058	0.129788	2.674852	6	-4.99139	-2.43079	-2.58313
6	-3.07712	1.17715	2.956988	1	-5.07609	-3.5121	-2.557
6	-4.12738	0.895861	3.848544	6	-6.14532	-1.64962	-2.68064
1	-4.82888	1.687416	4.09294	6	-6.05374	-0.25548	-2.65977
6	-4.30411	-0.37617	4.393491	1	-6.95354	0.350848	-2.69655
6	-3.43692	-1.41146	4.036321	6	-4.8042	0.375522	-2.58278
1	-3.58917	-2.41092	4.432165	6	-1.65937	0.401564	-3.71502
6	-2.36216	-1.17768	3.168218	1	-2.06137	1.254908	-4.27105
6	-0.02114	1.276248	2.054825	1	-1.79686	-0.50346	-4.31802
1	-0.32465	1.958013	2.851285	6	-0.23548	0.636542	-3.36831
1	0.083532	1.841651	1.124586	6	0.540901	0.027286	-2.39236
6	1.241819	0.599584	2.468195	1	0.274585	-0.69699	-1.63435
6	1.820854	-0.59261	2.062951	6	3.022126	0.298881	-1.82825
1	1.49498	-1.34518	1.364991	1	3.721642	-0.15508	-2.54034
6	3.964215	-1.76456	2.870176	1	2.812776	-0.44035	-1.05523
1	3.506746	-2.66454	3.288254	6	3.630942	1.512249	-1.19057
1	4.713653	-1.39864	3.579465	6	4.768312	2.812706	0.142575
6	4.585777	-2.13053	1.562093	6	5.525909	3.365169	1.181954
6	5.513106	-3.29568	-0.01519	1	5.871635	2.746156	2.001472
6	6.013938	-4.30546	-0.84684	6	5.79787	4.731152	1.127944
1	5.917359	-5.34641	-0.56014	1	6.379822	5.191808	1.918912
6	6.632947	-3.92522	-2.0372	6	5.324619	5.535306	0.065233

1	7.032636	-4.68513	-2.70071	1	5.557124	6.595007	0.060406
6	6.75818	-2.56327	-2.39746	6	4.561876	5.000981	-0.97396
1	7.2571	-2.30557	-3.32632	1	4.196608	5.623439	-1.78319
6	6.265248	-1.54259	-1.58187	6	-4.70165	1.894861	-2.4736
1	6.385767	-0.49842	-1.85081	1	-3.73585	2.235386	-2.86262
6	5.640058	-1.92911	-0.38921	1	-5.47094	2.344634	-3.11009
6	-1.46003	-2.33093	2.733388	6	4.293745	3.629495	-0.91752
1	-0.45718	-1.95146	2.525478	6	-3.89035	2.303648	-0.06975
6	-6.12257	3.000547	-0.68683	6	-4.90067	2.412462	-1.0509
1	-6.90128	3.095317	-1.43892	1	-2.51456	1.28423	-1.16397
6	-6.34567	3.476289	0.606549	1	4.860162	-0.18463	0.618354
6	-5.33737	3.34647	1.567319	1	-1.13451	-0.77408	0.579772
1	-5.50155	3.714037	2.576524	1	3.083344	2.967712	-2.61175
6	-4.11078	2.752445	1.250387	1	-3.69388	-6.00203	0.856649
6	-3.02515	2.560306	2.301248	1	-7.11683	-2.12771	-2.7528
1	-3.15577	3.318216	3.083314	1	-7.29103	3.942758	0.862837
1	-2.05968	2.734282	1.83056	1	-5.12424	-0.56461	5.078542

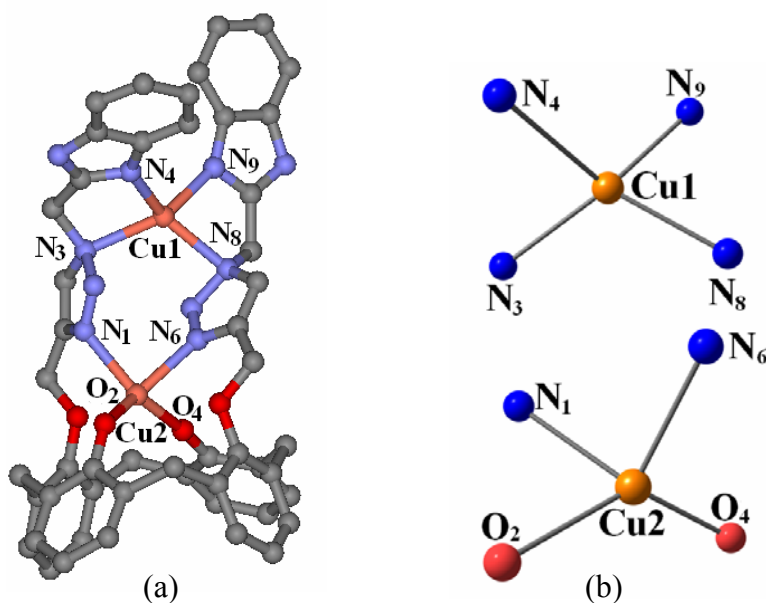
Table S6. Cartesian coordinates for B3LYP/6-31G(d,p) optimized structure of $[L'(Cu)]^{2+}$.



Z	Coordinates			Z	Coordinates		
	x	y	z		x	y	z
29	-3.07354	-0.07765	-0.12432	1	2.056772	2.614882	2.450787
8	2.097972	0.168334	2.151544	1	3.296158	3.652022	3.126106
8	2.106159	1.591073	-0.10121	6	3.056263	2.6223	-0.1468
8	2.206941	-0.47476	-2.22912	6	3.544354	3.271086	1.032138
8	2.651959	-1.80265	0.187981	6	4.449763	4.351922	0.884671
7	-1.55278	0.248052	2.942383	1	4.826618	4.849084	1.769565
7	-2.52861	0.77853	2.05578	6	4.85101	4.799359	-0.39226
7	-1.81974	1.253015	0.853885	6	4.364756	4.153099	-1.5488
7	-4.55397	3.761119	0.242206	1	4.676341	4.494417	-2.52772
7	-4.3232	1.606656	-0.28321	6	3.473966	3.057593	-1.44238
7	-0.02657	-2.07932	-1.58086	6	3.010145	2.303054	-2.69721
7	-1.2937	-2.19495	-1.04647	1	3.013584	2.987276	-3.54444

7	-2.18909	-1.20507	-1.76344	1	1.993588	1.951803	-2.54657
7	-5.15119	-3.42276	-1.05385	6	3.515689	-0.23078	-2.73146
7	-4.44223	-1.52483	-0.11049	6	3.92124	1.105926	-3.01149
6	3.362911	0.281138	2.786497	6	5.234409	1.306042	-3.51193
6	4.108111	-0.88506	3.122714	1	5.565175	2.309228	-3.74818
6	5.377901	-0.70204	3.732149	6	6.115519	0.216433	-3.68971
1	5.959698	-1.5705	4.013474	6	5.715319	-1.09075	-3.33286
6	5.894779	0.591822	3.963617	1	6.410207	-1.91511	-3.43215
6	5.167186	1.733592	3.559388	6	4.409737	-1.33693	-2.83718
1	5.583272	2.721941	3.708508	6	1.282301	-0.74427	-3.30331
6	3.892994	1.595673	2.955308	1	1.601877	-1.59125	-3.92505
6	1.01647	0.139514	3.106336	1	1.136144	0.123029	-3.95802
1	1.169322	0.861971	3.918774	6	-0.04501	-1.09714	-2.6253
1	0.91086	-0.85196	3.564189	6	-1.32048	-0.58532	-2.78928
6	-0.27711	0.493669	2.364956	1	-1.71827	0.157726	-3.47011
6	-0.37776	1.07927	1.11401	6	-3.35726	-2.03268	-2.31292
1	0.397826	1.4284	0.425522	1	-2.97928	-2.94953	-2.7757
6	-2.23727	2.69957	0.650695	1	-3.86297	-1.43281	-3.0774
1	-1.62246	3.165873	-0.12603	6	-4.32098	-2.35059	-1.16112
1	-2.12656	3.259924	1.583886	6	-5.86097	-3.30086	0.172839
6	-3.71196	2.694949	0.212638	6	-6.83072	-4.12698	0.788268
6	-5.8166	3.346237	-0.26173	1	-7.17477	-5.04346	0.324891
6	-7.03449	4.0425	-0.44285	6	-7.31722	-3.68999	2.040184
1	-7.13608	5.088529	-0.18063	1	-8.05967	-4.28845	2.555243
6	-8.10615	3.297507	-0.9813	6	-6.85388	-2.48667	2.645524
1	-9.06192	3.783171	-1.1396	1	-7.25191	-2.19519	3.610338
6	-7.96096	1.922958	-1.32058	6	-5.88846	-1.66685	2.024197
1	-8.80964	1.388792	-1.73095	1	-5.52512	-0.75595	2.484172
6	-6.7412	1.239653	-1.13493	6	4.003118	-2.73901	-2.35599
1	-6.63368	0.194111	-1.39065	1	2.922181	-2.84702	-2.40175
6	-5.66298	1.984784	-0.59353	1	4.429287	-3.47546	-3.03316
6	3.123475	2.823812	2.442921	6	-5.40126	-2.10335	0.764367
6	4.494755	-3.05379	-0.93252	6	3.824644	-2.55967	0.228863
6	5.6556	-3.84929	-0.75983	1	3.780817	-2.95364	3.618602
1	6.169548	-4.22924	-1.63369	1	2.537781	-2.26068	2.578641
6	6.13947	-4.16506	0.526983	1	2.310465	1.026666	0.6849
6	5.470076	-3.67461	1.66884	1	2.533552	-1.49028	-0.73961
1	5.839923	-3.91939	2.656381	1	-4.31948	4.693476	0.598717
6	4.315507	-2.86852	1.535765	1	-5.22678	-4.19572	-1.72373
6	3.6062	-2.29383	2.770389	1	7.113003	0.388189	-4.07468
1	5.53434	5.634009	-0.4834	1	7.022119	-4.78184	0.636797
1	6.864098	0.709183	4.431793				

Table S7. Cartesian coordinates for B3LYP/6-31G(d,p) optimized structure of $[L'_{-2H}(Cu)_2]^{2+}$.



Z	Coordinates			Z	Coordinates		
	x	y	z		x	y	z
8	1.594449	-0.24818	2.453721	6	6.318959	-3.71016	0.680041
8	2.262104	1.430794	-0.07618	6	5.551739	-3.36676	1.799803
8	2.242497	-0.21842	-2.35002	1	5.946452	-3.56119	2.796746
8	2.491663	-2.18311	0.241368	6	4.290371	-2.78421	1.670427
6	-0.53289	0.680941	1.978013	6	3.494398	-2.33684	2.891633
6	-1.77744	1.241318	1.989639	1	3.785642	-2.9498	3.75387
7	-2.08418	1.552113	0.656876	1	2.430932	-2.48963	2.699863
7	-5.09769	3.705632	0.398276	1	4.515159	6.147364	0.069331
7	-4.72926	1.606411	-0.2522	1	7.300735	0.639241	-3.45113
6	0.002886	-0.74132	-2.69857	1	7.291877	-4.17891	0.797798
6	-1.29549	-0.55807	-3.04619	1	6.300231	1.095303	4.395603
7	-2.09355	-1.11517	-2.02146	29	-3.234409	0.105082	-0.52373
7	-4.37559	-3.83554	-1.07274	1	-4.9007	4.641811	0.722039
7	-4.23564	-1.751	-0.30018	1	-4.17148	-4.64116	-1.64635
6	2.840486	0.163209	2.937685	29	1.552645000	-0.53053	-0.16864
6	3.755398	-0.86901	3.231077	1	-1.74105	-0.07528	-3.90367
6	4.994976	-0.50336	3.770712	1	-2.47028	1.454684	2.789986
1	5.709504	-1.28554	4.011277	6	-4.98889	-2.50194	0.598444
6	5.335528	0.833069	3.969959	6	3.732351	-2.56803	0.3672
6	4.453302	1.831235	3.564325	6	4.556676	-2.84395	-0.773
1	4.747793	2.875445	3.631223	6	5.814466	-3.4259	-0.59297
6	3.202441	1.524534	3.009814	1	6.414504	-3.67123	-1.46874
6	0.395458	0.169285	3.062602	1	1.198978	0.472879	-4.0225
1	0.565369	0.953952	3.810213	7	0.035984	-1.42378	-1.47389
1	-0.06879	-0.68749	3.575462	7	-1.15336	-1.71353	-1.0896
7	-0.10403	0.671488	0.664624	6	-3.07866	-2.14317	-2.44514
7	-0.95303	1.223902	-0.1126	1	-2.55787	-2.99709	-2.89594
6	-2.6953	2.858997	0.302001	1	-3.72749	-1.69341	-3.20511
1	-2.25307	3.139428	-0.66019	6	-3.88962	-2.57591	-1.26388

1	-2.40862	3.62117	1.032821	6	-5.08725	-3.82896	0.123125
6	-4.17861	2.72339	0.168451	6	-5.78189	-4.82344	0.814043
6	-6.35087	3.17827	0.09441	1	-5.8473	-5.84218	0.445481
6	-7.63852	3.716119	0.141245	6	-6.38514	-4.44487	2.011823
1	-7.8255	4.738426	0.454125	1	-6.93259	-5.18546	2.586069
6	-8.67996	2.870954	-0.2371	6	-6.29679	-3.12319	2.497854
1	-9.69844	3.245479	-0.21766	1	-6.78104	-2.87349	3.436635
6	-8.44295	1.540509	-0.64363	6	-5.60116	-2.13739	1.803314
1	-9.28591	0.91837	-0.92718	1	-5.53059	-1.12126	2.176674
6	-7.15654	1.010395	-0.68624	6	4.050778	-2.49105	-2.16946
1	-6.96957	-0.01344	-0.99127	1	2.961381	-2.57421	-2.17227
6	-6.09907	1.848298	-0.31255	1	4.451791	-3.21818	-2.8873
6	2.377977	2.681068	2.444818	6	3.096546	2.524251	-2.58415
1	1.367192	2.346099	2.208027	1	3.257884	3.252349	-3.38915
1	2.293067	3.458048	3.216337	1	2.055708	2.191072	-2.63901
6	2.828239	2.588565	-0.05075	6	3.588352	0.004695	-2.64705
6	2.959812	3.310646	1.187171	6	4.019884	1.332988	-2.8122
6	3.56118	4.569054	1.207035	6	5.371116	1.538479	-3.11632
1	3.647528	5.101297	2.154608	1	5.732664	2.55503	-3.24936
6	4.046742	5.16786	0.036906	6	6.256016	0.463917	-3.20856
6	3.901813	4.485575	-1.17859	6	5.812168	-0.83027	-2.93839
1	4.256004	4.953044	-2.09745	1	6.521149	-1.65317	-2.93754
6	3.302324	3.227565	-1.24903	6	4.471489	-1.09039	-2.61936
1	1.604747	-1.26149	-4.02629	6	1.30514	-0.4172	-3.3852

Table S8. Percentage of MOs present on the fragments of L' , $[L'(Cu)]^{2+}$ and $[L'_{-2H}(Cu)_2]^{2+}$ for different HOMO/LUMO which were generated by using Chemissian 1.77 software.

L'					
MOs	Energy eV	Cone	Triazole	Benzimidazole	Copper
HOMO – 1	-5.909	96	0	0	0
HOMO	-5.657	99	0	0	0
LUMO	-1.138	0	20	77	0
LUMO + 1	-0.886	0	67	31	0
$[L'(Cu)]^{2+}$					
HOMO (α) – 1	-10.276	100	0	0	0
HOMO (α)	-10.079	97	0	0	0
LUMO (α)	-7.598	0	95	0	0
LUMO (α) + 1	-7.282	0	91	0	0
$[L'_{-2H}(Cu)_2]^{2+}$					
HOMO – 1	-10.065	83	0	0	12
HOMO	-9.417	65	10	0	26
LUMO	-8.514	0	31	62	7
LUMO + 1	-7.030	0	74	16	8

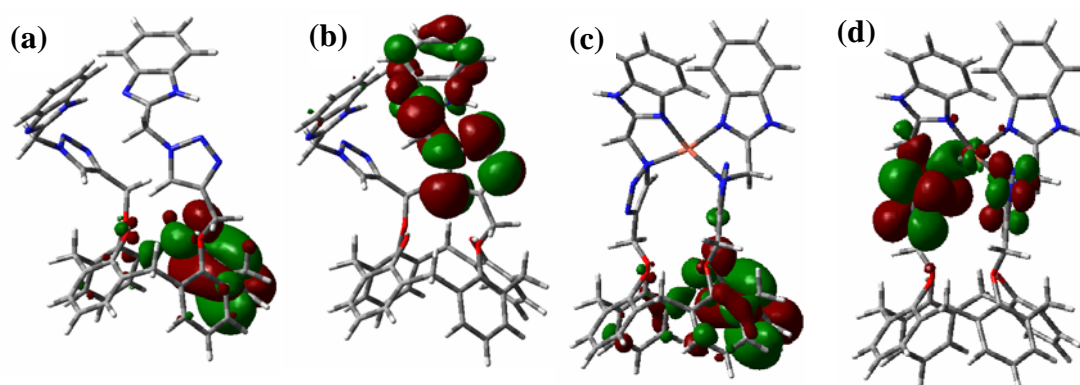


Figure S15: Pictorial representation of the molecular orbitals (MOs) present on different fragments of L and $[L'(Cu)]^{2+}$: (a) HOMO of L' ; (b) LUMO of L' ; (c) HOMO (α) of $[L'(Cu)]^{2+}$; (d) LUMO (α) of $[L'_{-2H}(Cu)_2]^{2+}$.